

# Applications of Microlensing to Stellar Astrophysics

Andrew Gould

Department of Astronomy, Ohio State University, Columbus, OH 43210, USA  
Laboratoire de Physique Corpusculaire et Cosmologie, Collège de France, 11 pl.

Marcelin Berthelot, F-75231, Paris, France

E-mail: gould@astronomy.ohio-state.edu

## ABSTRACT

Over the past decade, microlensing has developed into a powerful tool to study stellar astrophysics, especially stellar atmospheres, stellar masses, and binarity. I review this progress. Stellar atmospheres can be probed whenever the source in a microlensing event passes over the caustic (contour of infinite magnification) induced by the lens because the caustic effectively resolves the source. Broad-band observations of four events have yielded limb-darkening measurements, which in essence map the atmospheric temperature as a function of depth. And now, for the first time, spectroscopic observations of one event promise much richer diagnostics of the source atmosphere. In the past two years, a practical method has finally been developed to systematically measure the lens masses in microlensing events. This will permit a census of all massive objects, both dark and luminous, in the Galactic bulge, including low-mass stars, brown dwarfs, white dwarfs, neutron stars, and black holes. The method combines traditional ground-based photometry with astrometric and photometric measurements by the *Space Interferometry Mission (SIM)* in solar orbit. Using a related technique *SIM* can also obtain accurate ( $\lesssim 1\%$ ) mass measurement of a dozen or so nearby stars, thus enabling precision tests of stellar models. Binary lenses can give rise to dramatic and easily detectable microlensing signatures, even for large mass ratios. This makes microlensing a potentially powerful probe of the companion mass distribution, especially in the Galactic bulge where this function is difficult to probe by other techniques.

*Subject headings:* astrometry – gravitational lensing – stars:atmospheres – stars:masses

## 1. Brief History

While microlensing observations were originally proposed as a means to search for dark matter in the form of massive compact halo objects (Paczynski 1986), and have proved very effective for that purpose (Alcock et al. 1998, 2000c; Lasserre et al. 2000), they have also been directed from the outset toward the Galactic bulge (Udalski et al. 1993) where the vast majority of events were expected to be due to ordinary stars in the Galactic disk (Paczynski 1991; Griest et al. 1991) and the bulge itself (Kiraga & Paczynski 1994). The event rate reported by OGLE (Udalski et al. 1994) and MACHO (Alcock et al. 1997a) was substantially too high to be consistent with any axisymmetric model of the Galaxy (Gould 1994c; Kuijken 1997), or even with any plausible barred model (Binney, Bissantz, & Gerhard 2000). Hence, the importance of microlensing as a probe of Galactic structure was recognized almost from the beginning, leading the EROS collaboration (Derue et al. 1999) to extend their surveys from the Galactic bulge to the spiral arms.

By contrast, the subject of the present review (microlensing applications to stellar astrophysics) was initially much slower to develop. It is true that Refsdal (1964) first proposed using microlensing to measure stellar masses more than 3 decades ago, but the idea remained dormant until Paczynski (1995) resurrected it, and not a single candidate for such a measurement was identified in the literature until last year (Salim & Gould 2000). There is no mention in the literature that stellar atmospheres might lead to observable signatures until Witt (1995), and the initial emphasis was on using these effects to learn more about the lens (Loeb & Sasselov 1995; Gould & Welch 1996), rather than about the atmosphere of the source.

Despite its late start, this aspect of microlensing has witnessed enormous progress over the past five years, partly because of intensifying theoretical interest, but mainly because of the emergence of three groups (MACHO/GMAN, MPS, PLANET) who dedicate themselves to the intensive microlensing follow-up observations that are required to probe these effects. In this review, I first summarize the basics of microlensing (§ 2), and then cover three major topics, stellar mass measurements (§ 3), binary distribution functions (§5), and resolution of stellar atmospheres (§ 6). In the interval (§ 4), I give a brief introduction to binary microlensing.

## 2. Microlensing Basics

Microlensing occurs when a massive object (“the lens”) becomes closely aligned with a more distant luminous object (“the source”). General relativity predicts that a lens of mass  $M$  will deflect the light from the source by an angle  $\alpha = 4GM/bc^2$ , where  $b$  is the impact parameter of the light trajectory relative to  $M$ . This formula has been verified by Hipparcos measurements to be accurate to within 0.3% (Froeschle, Mignard & Arenou 1997). If the lens is a point mass (or more generally, spherical) and the lens and source are perfectly aligned with the observer, then there is axial symmetry, and the source is imaged into a ring of angular radius  $\theta_E$  (Einstein 1936), called the “angular Einstein ring”. Its projection onto the plane of the observer is called the “projected Einstein ring”,  $\tilde{r}_E$ . From simple geometric considerations (see Fig. 1), one immediately finds

$$\tilde{r}_E \theta_E = \frac{4GM}{c^2}, \quad \frac{\theta_E}{\tilde{r}_E} = \frac{\pi_{\text{rel}}}{\text{AU}}, \quad (1)$$

where  $\pi_{\text{rel}}$  is the lens-source relative parallax. These are easily solved,

$$\theta_E = \sqrt{\kappa M \pi_{\text{rel}}}, \quad \pi_E \equiv \frac{\text{AU}}{\tilde{r}_E} = \sqrt{\frac{\pi_{\text{rel}}}{\kappa M}},$$

$$\kappa \equiv \frac{4G}{c^2 \text{AU}} \simeq \frac{8 \text{ mas}}{M_\odot}, \quad (2)$$

where the “microlens parallax”  $\pi_E$  contains the same information as  $\tilde{r}_E$  but in a more convenient form.

In the more general case, the source is not perfectly aligned with the lens, so the axial symmetry is broken. After a small bit of algebra, one finds that the angular separation between the source and the lens ( $\theta_{\text{rel}} = \theta_s - \theta_l$ ) and the angular separation between the image and the lens ( $\theta_I$ ) are related by

$$\theta_I^2 - \theta_I \theta_{\text{rel}} = \theta_E^2, \quad \frac{\theta_{I\pm}}{\theta_E} = \frac{u \pm \sqrt{u^2 + 4}}{2}, \quad u \equiv \frac{\theta_{\text{rel}}}{\theta_E}, \quad (3)$$

which implies that there are two images, one on either side of the lens. Since for typical bulge events  $\pi_{\text{rel}} \sim 0.04 \text{ mas}$ , the image separations,  $\sim 2\theta_E \lesssim 1 \text{ mas}$ , are far smaller than can be resolved with any existing instrument. Hence, the only microlensing effect that has been observed to date is the magnification,  $A$ . By Liouville’s theorem, surface brightness is conserved, so  $A$  is equal to the ratio of

the area of the image to that of the source. For small sources, this is given by the Jacobian of the transformation implied by equation (3). Combining both image magnifications,  $A = A_+ + A_-$ , one finds

$$A_{\pm} = \frac{A \pm 1}{2}, \quad A = \frac{u^2 + 2}{u\sqrt{u^2 + 4}}. \quad (4)$$

If the observer, source, and lens are all in rectilinear motion, then  $u$  varies according to the Pythagorean theorem

$$u = \sqrt{u_0^2 + \frac{(t - t_0)^2}{t_E^2}}, \quad t_E \equiv \frac{\theta_E}{\mu_{\text{rel}}}, \quad (5)$$

where  $t_0$  is the time of closest approach,  $u_0 = u(t_0)$ ,  $t_E$  is the ‘‘Einstein timescale’’, and  $\mu_{\text{rel}}$  is the amplitude of the lens-source relative proper motion. Thus, three parameters determine a standard microlensing event,  $t_0$ ,  $u_0$ , and  $t_E$ . This is both a blessing and a curse: a blessing because the simplicity of microlensing light curves allows them to be robustly distinguished from other much more common forms of stellar variability, and a curse because only three parameters can be recovered from a normal microlensing event. Moreover, the only one of these parameters that carries any information about the lens,

$$t_E = \frac{\sqrt{\kappa M \pi_{\text{rel}}}}{\mu_{\text{rel}}}, \quad (6)$$

is a complicated combination of the lens mass, and the lens and source distances and transverse velocities.

### 3. Masses of Microlenses

#### 3.1. Bulge Lenses

Thus it was always recognized that microlensing surveys would not yield mass measurements for individual events. The best one could hope for would be statistical statements based on the observed distribution of timescales, equation (6), and assumptions about the underlying distributions of  $\pi_{\text{rel}}$  and  $\mu_{\text{rel}}$  (Mao & Paczyński 1996). Early efforts to apply this approach to bulge events by Zhao, Spergel, & Rich (1995) and Han & Gould (1996) revealed two types of problems. First, there

were an excess of short events ( $t_E \lesssim 10$  days) relative to what one would expect if the bulge mass function (MF) were similar to the local disk MF measured from *HST* star counts (Gould, Bahcall, & Flynn 1997), and second there was also an excess of long events ( $t_E \gtrsim 50$  days). Alternatively, one could characterize the situation as problems in the normalization and shape of the timescale distribution: there are too many events overall, and too many in the wings relative to the center. A later and more thorough analysis by Peale (1998) continued to show a strong excess of short events over what could be expected from lower main-sequence stars if the MF were similar to the local one, although Peale (1999) argued that if the bulge contained a population of brown dwarfs similar to the local one discovered by 2MASS, there would actually be a deficit of short events.

Han (1997) argued that much of the short-event excess could be explained as due to events with intrinsically faint sources which found their way into the surveys by “amplification bias”, and whose timescales were consequently being systematically underestimated. Zoccali et al. (2000) used NICMOS on *HST* to measure the bulge MF down to  $0.15 M_\odot$  and found that it indeed contains far more low-mass stars than the local MF of Gould et al. (1997), and therefore should give rise to more short events.

Nevertheless, when Alcock et al. (2000b) applied a more sophisticated image differencing analysis to MACHO bulge data, which should have removed the effects of amplification bias, the twin inconsistencies (normalization and shape) between the observed and predicted timescale distributions remained basically intact, albeit at a reduced level. Moreover, an analysis of a largely independent data set of MACHO bulge clump giants by Popowski et al. (2001) confirms both the excess of long events and the resulting high optical depth that Binney et al. (2000) found so difficult to reconcile with models.

However, as shown in Figure 2, there is a fundamental limit to how much information about the MF can be extracted from microlensing timescales alone. Panel (a) shows a plausible bulge MF decomposed into main-sequence stars and brown dwarfs (MS+BDs), white dwarfs (WDs), neutron stars (NSs), and black holes (BHs). The MS MF in the range  $0.15 M_\odot < M < 0.9 M_\odot$  is taken from actual measurements by Zoccali et al. (2000), but the other components are based on Gould’s (2000b) conjectures. In particular, the cut off in the BD MF at  $0.03 M_\odot$  is fairly arbitrary. Panel (b) shows the distribution of timescales expected for microlensing events of fixed lens mass,  $M = M_\odot$ , towards a field at projected distance,  $b$ , from the Galactic

center and assuming an isotropic bulge velocity dispersion,  $\sigma$ . The normalization of the timescale distribution is  $t_{bM_\odot} \equiv (2GM_\odot/b)^{1/2}/\sigma c$ . The timescale distribution is shown as a function of  $t_E^2$  rather than  $t_E$  to make it directly comparable to the MF, since for fixed  $\pi_{\text{rel}}$  and  $\mu_{\text{rel}}$ ,  $M \propto t_E^2$  (see eq. 6). Note that the FWHM of this distribution is a factor  $\sim 100$ . Since this is larger than the full extent of the MF in Panel (a), it follows that one can learn very little about the MF beyond its mean and variance from timescale observations alone, even assuming that the bulge velocity distribution and “contamination” from foreground disk lenses were understood perfectly. This conclusion is illustrated in Panel (c), which gives the predicted distribution of timescales formed by convolving Panels (a) and (b). Note that all of the sharp features in Panel (a) are utterly obliterated, so that it is impossible to pick out BDs, WDs, NSs, or BHs individually or even statistically. Thus, although finding the mean and variance of the MF would be very important, and in particular would provide the only clue we have as to the BD cutoff in the bulge, all of the detailed information about the large numbers (several hundred to date) of dark (BD, WD, NS, BH) lenses being detected toward the bulge would be lost.

The solution is to find the lens masses and distances for individual events. Both  $M$  and  $\pi_{\text{rel}}$  can be determined if  $\theta_E$  and  $\tilde{r}_E$  are measured (see eq. 1). Fortunately, these two quantities are both “observables”:  $\theta_E$  can be measured if it can be compared to some “standard angular ruler” in the plane of the sky, and  $\tilde{r}_E$  can be measured if it can be compared to some “standard physical ruler” in the plane of the observer. See my earlier review (Gould 1996) for the large number of ideas to measure  $\theta_E$  and  $\tilde{r}_E$  in various circumstances. A few new ideas have been advanced since then (Han & Gould 1997; Hardy & Walker 1995; Gould & Andronov 1999; Honma 1999). Unfortunately, to date there have been only about a half dozen measurements each of  $\theta_E$  (Alcock et al. 1997b,2000a; Albrow et al. 1999a,2000,2001a; Afonso et al. 2000) and of  $\tilde{r}_E$  (Alcock et al. 1995; Bennett et al. 1997; Mao 1999, Soszyński et al. 2001). In no case have both been measured for the same event, so that to date there is not a single lens mass measurement. The problem is that the two standard rulers that have been applied, the angular size of the source (Gould 1994a; Nemiroff & Wickramasinghe 1994; Witt & Mao 1994) which is known from its dereddened color and magnitude and the color/surface-brightness relation (van Belle 1999), and the physical size of the Earth’s orbit (Gould 1992), are available only for very special, almost non-intersecting, subclasses of events. These are respectively, caustic-crossing and very long ( $t_E \gtrsim 90$  days) events.

However, work over the last five years has developed a practical method to obtain both  $\theta_E$  and  $\tilde{r}_E$  for a large and representative sample of events. First, Hog, Novikov & Polnarev (1995), Walker (1995), and Miyamoto & Yoshii (1995) showed that  $\theta_E$  can in principle be determined from precision measurements of the *centroid* of the two lensed images,  $\vec{\theta}_c \equiv (A_+\vec{\theta}_{I+} + A_-\vec{\theta}_{I-})/A$ . Boden, Shao, & Van Buren (1998) and Paczyński (1998) then showed that the proposed *Space Interferometry Mission (SIM)* would be capable of making such measurements. From equations (3) and (4), the astrometric shift  $\delta\vec{\theta}_c$  of the centroid relative to the position of the source in the absence of lensing is given by,

$$\delta\vec{\theta}_c \equiv \vec{\theta}_c - \vec{\theta}_{\text{rel}} = \frac{\vec{\theta}_{\text{rel}}}{u^2 + 2}. \quad (7)$$

Although it is not immediately obvious from equation (7), if  $\vec{\theta}_{\text{rel}}$  moves in a straight line, then  $\delta\vec{\theta}_c$  traces an ellipse, and its maximum amplitude (at  $u = 2^{1/2}$ ) is  $\theta_E/8^{1/2}$ . Recall from the discussion following equation (3) that  $2\theta_E \lesssim 1$  mas, so that the two images cannot be resolved. However, it is much easier to centroid an image than resolve it, and in particular *SIM* is expected to reach an astrometric precision of  $\sim 4 \mu\text{as}$ . Miyamoto & Yoshii (1995), Boden et al. (1998), and Paczyński (1998) also noted that the motion of the Earth would cause  $\vec{\theta}_{\text{rel}}$  to deviate from a straight line, and so induce distortions on the ellipse, in principle permitting the measurement of  $\tilde{r}_E$ , and so of  $M$ , using astrometry alone. However, it turns out that these parallax distortions are unmeasurably small in most cases, as shown both analytically and numerically by Gould & Salim (1999).

Nevertheless, simultaneous measurement of  $\tilde{r}_E$  and  $\theta_E$  should be possible for a large number of events using *SIM*. From equation (2), and recalling that  $\pi_{\text{rel}} \sim 0.04$ , it follows that  $\tilde{r}_E \lesssim 10$  AU. Hence, the event will have substantially different parameters if viewed from a satellite in Earth-trailing orbit ( $t_{0,\text{sat}}, u_{0,\text{sat}}, t_{E,\text{sat}}$ ) than it does from the Earth ( $t_{0,\oplus}, u_{0,\oplus}, t_{E,\oplus}$ ). One can then determine  $\vec{\pi}_E$  up to a four-fold degeneracy (Refsdal 1966),

$$\vec{\pi}_E = \frac{\text{AU}}{|\mathbf{D}_{\text{sat}}|} \left( \frac{\Delta t_0}{t_E}, \Delta u_0 \right), \quad \Delta t_0 \equiv t_{0,\text{sat}} - t_{0,\oplus}, \quad \Delta u_0 \equiv \pm |u_{0,\text{sat}} \pm u_{0,\oplus}|, \quad (8)$$

where  $\mathbf{D}_{\text{sat}}$  is the Earth-Satellite separation vector projected onto the plane of the sky, and the direction of  $\vec{\pi}_E$  is taken to be that of the lens-source relative proper motion,  $\vec{\mu}_{\text{rel}}$ , with  $\mathbf{D}_{\text{sat}}$  defining the  $x$ -axis. See Figure 5 from my previous review (Gould 1996).

The four-fold degeneracy arises because one does not know on which side the source passes the lens and hence whether  $u_{0,\text{sat}}$  and  $u_{0,\oplus}$  should be regarded effectively as “positive” or “negative”. See Figures 2 and 3 from Gould (1994b). However, this degeneracy can usually be resolved by measuring the small difference,  $\Delta t_E = (t_{E,\text{sat}} - t_{E,\oplus})$ , which is proportional to  $\Delta u_0$  (Gould 1995; Boutuereux & Gould 1996; Gaudi & Gould 1997a).

Gould & Salim (1999) pointed out that since *SIM* does astrometry by *counting* photons as a function of fringe position, it can simultaneously do photometry and hence can (in conjunction with ground-based photometry) measure  $\vec{\pi}_E$ . Moreover, since the axis of the astrometric ellipse described by equation (7) is parallel to  $\vec{\mu}_{\text{rel}} = -d\vec{\theta}_{\text{rel}}/dt$ , *SIM* astrometry provides a second method to distinguish among the four solutions given by equation (8), which each would imply different directions for  $\vec{\pi}_E$  (and hence  $\vec{\mu}_{\text{rel}}$ ). Finally, since *SIM* automatically measures  $\pi_s$  and  $\vec{\mu}_s$ , the parallax and proper motion of the source, it can also determine  $\pi_l = \pi_{\text{rel}} + \pi_s$  and  $\vec{\mu}_l = \vec{\mu}_{\text{rel}} + \vec{\mu}_s$ , the parallax and proper motion of the lens. Salim & Gould (2000) showed that for bright ( $I \sim 15$ ) sources, *SIM* could measure  $M$  accurate to  $\sim 5\%$  in 5 hours of observation time, which is approximately the resolution of the mass function illustrated in Figure 2.

Han & Kim (2000) have proposed another method to measure  $\tilde{r}_E$  by comparing *SIM astrometry* to that of ground-based interferometers. The principle is broadly similar to the above *photometric* comparison, but in this case there is no degeneracy.

Such a MF measurement would automatically yield substantial information about the rate of binarity and the distribution of binary mass ratios. Although a large fraction of stars are believed to be in binaries, for a binary to be recognizable from a microlensing light curve, its projected separation must be close to  $\theta_E$  (see § 4). As a result, only  $\sim 5\text{--}10\%$  of microlensing events are photometrically distinguishable from point lenses. However, in a series of paper, C. Han and his collaborators have demonstrated that a much larger fraction of binaries can be detected and accurately characterized astrometrically (Chang & Han 1999; Han, Chun & Chang 1999; Gould & Han 2000; Han 2001).



### 3.2. Nearby Lenses

Refsdal (1964) showed that it would be possible to determine the mass of a nearby star by measuring its deflection of light from a more distant field star. While the mathematics for this type of microlensing are formally identical to those described in § 3.1, the physical conditions, observational requirements, and scientific motivations all differ radically. Because the astrometric microlensing effect falls off only as  $u_0^{-1}$  (compared to  $u_0^{-4}$  for the photometric effect) the encounters typically have  $u_0 \gg 1$ . Hence, the photometric effect is negligible, and only the astrometric effect survives (Miralda-Escudé 1996). In this regime, the source appears displaced by  $\alpha' = \kappa M \pi_{\text{rel}} / \theta_{\text{rel}}$ , and the ellipsoidal path of deviation becomes circular. Since the lens and source are both luminous, their relative separation and parallax,  $\theta_{\text{rel}}$  and  $\pi_{\text{rel}}$  are measurable astrometrically, and hence  $M$  can be inferred directly from the measurement of  $\alpha'$  (together with a time series of measurements to determine  $\pi_{\text{rel}}$  and  $\theta_{\text{rel}}$ ). Second, the motivation for doing these observations is not the cataloguing of dark objects, but the precision measurement of the mass of luminous ones. This is the only practical method to obtain accurate masses for single stars (except the Sun), and as we shall see below, the method is strongly biased toward metal-poor stars (because of their high proper motions) for which there are at present no reliable mass measurements at all. Thus, it is complementary to the standard techniques for measuring stellar masses using visual and eclipsing binaries (e.g. Henry & McCarthy 1993).

This idea remained dormant for 30 years until Paczyński (1995) resurrected it. It was further studied in the context of the accurate measurements possible using *SIM* and *Global Astrometric Interferometry for Astrophysics (GAIA)* by Miralda-Escudé (1996), Paczyński (1998), and Dominik & Sahu (2000). Given an astrometric instrument of sufficient precision, the central problem is the identification of lens-source pairs that will come close enough to permit an accurate mass measurement. In principle, one would like to consider all possible pairs of stars on the sky, but this is not possible with existing catalogs because these lack proper motions for most stars. Hence a more focused approach is required.

For a fixed amount of observing time to be scheduled during a fixed project lifetime, the probability that a given nearby star can have its mass measured to a given fractional precision is approximately,

$$P \propto \pi_l \mu_l M N_s, \tag{9}$$

where  $N_s$  is the density of sources behind the lens. Hence, nearby, high proper motion stars close to the Galactic plane have the best chance. Since nearby stars also tend to have high proper motions, Paczyński (1998) advocated checking the paths of proper-motion stars for future encounters with background sources, and specifically estimated that *Hipparcos* catalog stars should have dozens of such encounters. Sahu et al. (1998) predicted three encounters by tracking the future paths of 500 high proper motion WDs on archival sky survey plates complemented with ground-based observations, although they did not identify these explicitly.

Gould (2000a) and Salim & Gould (2000) outlined a three step procedure to systematically find candidates by combining a proper-motion catalog, e.g. *Hipparcos* or Luyten (1979,1980, hereafter NLTT) with an all-sky position catalog, e.g., USNO-A (Monet et al. 1998). First, estimate the lens distance using parallax for *Hipparcos* stars or a reduced proper motion diagram for NLTT stars. Since the mass error scales as the distance squared, the list of possible candidates would mushroom without this step. Second, search in the neighborhood of the *future* path of these stars for sources whose *archival* (e.g. 1950) USNO-A positions put them close enough for a significant deflection. Third, make follow-up observations of the lens-source pairs to confirm their encounter parameters. The third step is required for three reasons: 1) the USNO-A positions are accurate only to 250 mas, which can be a significant fraction of the impact parameter in some cases, 2) the source stars will have moved due to their (unknown) proper motions, which are generally expected to be of order 2 mas/yr, but could be larger, 3) the NLTT proper motions are accurate only to 20 mas/yr, which implies an error in 2010 position of 1.''2.

Salim & Gould (2000) carried out this search through the second step. They found 11 encounters for *Hipparcos* stars during the interval 2005-2015 for which 1% mass measurements could be obtained in less than 14 hours of *SIM* time. The errors in 2010 positions due to reasons (1) and (2) above were not expected to be large for these stars. Salim & Gould (2000) also produced a table of 180 NLTT stars for follow-up observations among which they expected  $\sim 10$  will have mass errors comparable to the 11 *Hipparcos* stars. The large errors in NLTT proper motions are responsible for this huge ratio of stars requiring follow-up to those that will be found useful. Salim & Gould (2001) are undertaking these follow-up observations.

What improvements can be hoped for in the future? These would come mainly from rectifying four shortcomings in the present catalogs. First, NLTT is nominally complete only for  $V \lesssim 18.5$ ,  $\delta > -20^\circ$ , and  $|b| > 10^\circ$ . Second, NLTT proper motions

are accurate only to 20 mas/yr, implying a barely acceptable error of  $1''.2$  in the predicted position of the encounter. Third, NLTT archival positions are accurate only to a few arcseconds, making them essentially useless for predicting encounters. This problem can be circumvented for  $\delta > -15^\circ$  by identifying NLTT stars on USNO-A, but fourth, USNO-A is missing essentially all NLTT stars for  $\delta < -15^\circ$ . Fifth, USNO-A lacks proper motions, so that encounters with slow nearby stars cannot be accurately predicted.

Some, but not all of these problems will be resolved with the publication of either of two projected all-sky position and proper motion surveys, USNO-B (D. Monet 1999, private communication) or Guide Star Catalog II (Baruffolo, Benacchio, & Benfante 1999). These are expected to go a magnitude deeper than NLTT, to have accurate positions and proper motions, and to cover the whole sky. However, the dearth of high-proper motion stars in southern catalogs derives fundamentally from the lack of coeval 2-color surveys in this region of the sky, which renders difficult their identification. Since no additional surveys are planned, this problem may persist.

In summary, with some additional work, one can expect perhaps a few dozen encounters per decade.

#### 4. Binary Microlensing

The other applications that I describe all make use of binary microlenses, i.e., microlensing where the mass distribution is composed of two point masses. Binary microlensing is one of the most active fields in microlensing today. In part this is due to the mathematical complexity of the subject and in part to the demands that are being placed on theory by new, very precise observations of binary events. Chang (1981) made the first study of binary microlenses in her thesis, which included a detailed investigation of the important limiting case of a high-mass ratio (“planetary”) binary. See also Chang & Refsdal (1979,1984). Schneider & Weiss (1986) made a comprehensive study of binary lenses despite the fact that they never expected any to be detected (P. Schneider 1994, private communication), in order to learn about caustics in quasar macrolensing. Indeed caustics are the main new features of binaries relative to point lenses. These are closed curves in the source plane where a point source is infinitely magnified. The curves are composed of 3 or

more concave segments that meet at cusps. Binary lenses can have 1, 2, or 3 closed caustic curves. If the two masses are separated by approximately an Einstein radius, then there is a single 6-cusp caustic. If they are separated by much more than an Einstein ring, then there are two 4-cusp caustics, one associated with each member of the binary. If the masses are much closer than an Einstein ring, there is a central 4-cusp caustic and two outlying 3-cusp caustics. Figure 3 shows two cases of the 6-cusp caustic, one close to breaking up into the two caustics characteristic of a wide binary and the other close to breaking up into the three caustics characteristic of a close binary. See also Schneider, Ehlers & Falco (1992). Witt (1990) developed a simple algorithm for finding these caustics. Multiple-lens systems can have even more complicated caustic structures (Rhie 1997; Gaudi, Naber, & Sackett 1998).

#### 4.1. Binary Lens Parameters

Recall from equation (5) that a point-lens light curve is defined by just three parameters,  $t_0$ ,  $u_0$ , and  $t_E$ . These three generalize to the case of binaries as follows:  $u_0$  is now the smallest separation of the source relative to the center of mass (alternatively geometric center) of the binary,  $t_0$  is the time when  $u = u_0$ , and  $t_E$  is the timescale associated with the combined mass of the binary. At least three additional parameters are required to describe a binary lens: the angle  $\alpha$  at which the source crosses the binary axis, the binary mass ratio  $q$ , and the projected separation,  $d$ , of the binary in units of the Einstein ring. Several additional parameters may be required in particular cases. If caustic crossings are observed, then the infinite magnification of the caustic is smeared out by the finite size of the source, so one must specify  $\rho_* = \theta_*/\theta_E$ , where  $\theta_*$  is the angular size of the source. If the observations of the crossing are sufficiently precise, one must specify one or more limb-darkening coefficients for each band of observation (see § 6.1). Finally, it is possible that the binary’s rotation is detectable in which case one or more parameters are required to describe it (Dominik 1998; Albrow et al. 2000). In addition, binary light curves often have data from several observatories in which case one needs two parameters (source flux and background flux) for each observatory.

## 4.2. Generic Caustic Crossings

Most stars are believed to be in binaries, but only of order 5–10% of microlensing events show recognizable signatures of binarity (e.g. Alcock et al. 2000a). The reason is simple: binaries span about 7 decades in semi-major axis, but unless their projected separation is within a factor  $\sim 3$  of  $\theta_E$ , the caustics are extremely small and the magnification patterns closely resemble those of isolated lenses (e.g. Di Stefano & Mao 1996; Gaudi & Gould 1997b). As a result, most detected binaries are drawn from the relatively small subclass with caustics whose dimensions are of order  $\theta_E$ . Since typically,  $10^{-3} \lesssim \rho_* \lesssim 10^{-2}$ , this implies that the source is generally several orders of magnitude smaller than the caustic, so that the caustic crossing usually takes place well away from any cusps.

A source inside a caustic will be imaged into five images, while outside the caustics it will be imaged into three images. Hence, at the caustic two images appear or disappear. These images are infinitely magnified. In the immediate neighborhood of a caustic (assuming one is not near a cusp), the magnification of the two new images diverges as  $A_2 \propto (-\Delta u_\perp)^{-1/2}$ , where  $\Delta u_\perp$  is the perpendicular separation of the source from the caustic (in units of  $\theta_E$ ). On the other hand, the three other images are unaffected by the approach of the caustic, so  $A_3 \sim \text{const}$ . Hence, the total magnification is given by (Schneider & Weiss 1987)

$$A = A_2 + A_3 \simeq \left( -\frac{\Delta u_\perp}{u_r} \right)^{-1/2} \Theta(-\Delta u_\perp) + A_{cc}, \quad (10)$$

where  $u_r$  is a constant that characterizes the approach to the caustic,  $A_{cc}$  is the magnification just outside the caustic crossing, and  $\Theta$  is a step function. For a source of uniform brightness, or limb darkened in some specified way, one can therefore write a relatively simple expression for the total magnification as a function  $\Delta u_\perp$  (Albrow et al. 1999b; Afonso et al. 2000).

## 5. Binary Companion Distribution

Microlensing can potentially probe the distribution of binary companions of bulge stars as a function of mass ratio and, to a certain extent, separation. These binary distribution functions provide one of the major observational constraints on theories of star formation. Since the Galactic bulge is the nearest elliptical/bulge

type structure, and since these are thought to contain the majority of stars in the universe, it is of exceptional importance to understand the distribution of binaries in this population.

I mentioned in § 3.1 that SIM astrometry would automatically yield substantial information about bulge binaries. However, a lot of work can already be done today using ground-based photometry. Alcock et al. (2000a) have conducted the only systematic search for binarity to date. Their study reveals both the promise and the pitfalls of this technique. On the one hand, caustic-crossing binaries yield an unambiguous signature, and microlensing is sensitive to companions of very small mass. On the other hand, there are a large number non-caustic crossers that are either not recognizable at all as binaries (see § 4.2) or whose binary parameters are poorly determined. Of course, one could adopt the approach of simply excluding these from the sample (and modeling the selection function accordingly) but Afonso et al. (2000) showed that for one caustic crossing binary with extremely good light-curve coverage, it was not possible to definitively distinguish between two sets of binary parameters, one where the companion was much heavier than the main perturber and separated from it by much more than an Einstein radius, and other where the companion was lighter than the main perturber and closer to it than an Einstein radius. At about the same time, Dominik (1999) showed that such wide/close degeneracies were generic to binary microlensing, although this degeneracy does appear to be breakable in many individual cases (e.g., Albrow et al. 2001a). Hence, careful modeling will be required to go from microlensing detections of binaries to a mass-ratio distribution.

Another problem (see § 4.2) is that photometric microlensing is mainly sensitive to binaries only over about a decade of projected separation: outside this range the great majority of binary events are indistinguishable from those due to a single lens. By searching for relatively rare events, this range can be extended only about another decade (Di Stefano & Mao 1996; Gaudi & Gould 1997b), compared to the  $\sim 7$  decades that binaries are known to populate (Duquenois & Mayor 1991). Nevertheless, microlensing could be combined with a variety of other techniques to probe all but about a decade in separations of bulge microlenses (Gould 2000b). Microlensing would be most sensitive to low-mass companions while other methods would provide most of the information about the separation distribution.

## 6. Stellar Atmospheres

The Sun appears brighter and bluer at its center than at its limb because the surface of last scattering lies deeper in the Sun where the atmosphere is hotter. Hence, by measuring the solar profile in various broad bands or spectral lines, one can learn about the atmosphere as a function of height. However, it has proven extremely difficult to make similar measurements for any star except the Sun, simply because they are unresolved or, at best, barely resolved. Caustic-crossing microlensing events permit such resolution because, as the caustic passes over the face of the star, different sections are strongly magnified at different times.

### 6.1. Limb-Darkening Measurements

At one time, it was thought that broad-band profiles, i.e., limb darkening (LD), could be measured from eclipsing binaries (e.g. Wilson & Devinney 1971; Twigg & Rafert 1980), but Popper (1984) showed that the LD coefficients derived in this manner were too large to be of use due to degeneracies with other parameters. In contrast to stellar eclipses, planetary transits such as HD 209458 can yield accurate LD measurements (Jha et al. 2000; Deeg, Garrido & Claret 2001). However, apart from the Sun and HD 209458 (both G dwarfs), and from the four microlensing measurements described below, there has been only one modern published LD measurement (Burns et al. 1997), which was of Betelgeuse and was carried out by means of interferometry. The paucity of LD measurements (as opposed to detections that could in principle be used to make measurements) may be due in part to an underappreciation of their importance. I will return to this point below.

Witt (1995), Valls-Gabaud (1995), and Bogdanov & Cherepashchuk (1995) showed that microlensing light curves could be affected by LD, but early papers on this subject (e.g., Loeb & Sasselov 1995; Gould & Welch 1996) were primarily concerned with using this effect to learn more about the lens rather than the source. Moreover, theoretical analysis was initially focused on source resolution by point-mass lenses whereas, as we shall see below, all four measurements made to date use binary microlenses. Gaudi & Gould (1999) have studied the signal-to-noise properties of light curves resulting from source transits of both point-lens caustics and binary fold caustics. Rhie & Bennett (1999) have systematically investigated the observational requirements for accurately measuring LD parameters from fold-caustic

crossings for a range of parameterizations.

Alcock et al. (1997b, the MACHO/GMAN collaboration) made the first microlensing detection of LD using the event MACHO 95-BLG-30, in which an M4 giant source ( $\sim 60 R_{\odot}$ ) was lensed by a point mass. However, the modest significance of the detection did not permit a measurement of LD parameters.

Albrow et al. (1999a, the PLANET Collaboration) made the first microlensing LD measurement using the event MACHO 97-BLG-28<sup>1</sup>, whose source they found spectroscopically to be a K2 giant. Both the event and the analysis were spectacular<sup>2</sup>, with the result that this is the best LD measurement to date. The event was extraordinary in that it had a cusp crossing, which is a priori very unlikely (see § 4.2). This makes the event both more difficult to monitor intensively, and more interesting. Cusp crossings are more difficult because they usually occur with little or no warning, so the onset of the crossing must be recognized in real time. In fact, both the PLANET and MACHO/GMAN collaborations alerted on the crossing within hours of its start. They are more interesting because the needle-like geometry of cusps makes them more similar to the point-like caustics of point-masses than to ordinary (fold) caustic crossings of binaries. Gaudi & Gould (1999) showed that point caustics were potentially much more sensitive probes of stellar structure than fold caustics, but argued that they were also much less likely to be observed.

The resulting intensive and accurate photometry from 3 sites, together with the needle geometry of the cusp, enabled Albrow et al. (1999a) to make 2-parameter LD models of the source in  $V$  and  $I$ , the only 2-parameter measurement using microlensing to date. They found overall excellent agreement with models of a K2 source by van Hamme (1993) and Días-Cordovas, Claret & Giménez (1995).

Afonso et al. (2000) made intensive observations of the binary fold-caustic event MACHO 98-SMC-1, primarily to determine whether the lens was in the Galactic halo (and so a contributor to the dark matter) or in the SMC itself. They found the latter, and in the course of doing so also obtained 1-parameter LD coefficients in  $V$ ,  $R$ , and  $I$ . The source was a metal-poor A dwarf. It is difficult to see how LD

---

<sup>1</sup>So named because it was the 28th event alerted by the MACHO collaboration toward the Galactic bulge in 1997. See <http://darkstar.astro.washington.edu/>

<sup>2</sup>Since I am so enthusiastic about this work, and since I am a co-author on many Albrow et al. papers, I should make clear that I had absolutely no connection with this one.



measurements could be made of such a star by any method except microlensing, since there are few, if any, in the Galaxy. Afonso et al. (2000) could not find models with which to compare their results.

Albrow et al. (2000) obtained 1-parameter LD coefficients in  $I$  band for the extremely complicated binary event MACHO 97-BLG-41 in which a cool K giant source ( $T \sim 5000$  K) crossed two disjoint caustics. That is, there were a total of 4 caustic crossings, including 3 fold caustics and one cusp. The main interest in this event is that it was the first for which binary rotation was measured. The caustic crossings were either missed or poorly covered, primarily due to bad weather. As a consequence, the LD measurement had rather large ( $\sim 20\%$ ) errors, so that while it was consistent with the models of Claret, Díaz-Cordovés & Giménez (1995), it could not challenge these models.

Finally, Albrow et al. (2001a) obtained 1-parameter LD coefficients in  $V$  and  $I$  bands of the fold-caustic crossing event OGLE 99-BUL-23<sup>3</sup>. Based on the source’s position in the color-magnitude diagram, they estimated it to be a G/K subgiant ( $T \sim 4800$  K).

Albrow et al. (2001a) developed for the first time the methods needed to use microlensing LD measurements to distinguish between competing models of stellar atmospheres. First, they made a much more thorough investigation of the errors in the LD coefficients. Whereas previous studies (Afonso et al. 2000; Albrow et al. 2001a) had quoted LD errors derived by fitting the light curve at fixed lens parameters, Albrow et al. (2001a) included the errors due to correlations with other parameters, and found in particular that the largest contribution came from correlation with the lens geometry ( $d, q$ ). Second, they made their comparison with published atmosphere models in the  $2$ -dimensional ( $V, I$ ) plane, which allowed them to take account of correlations between these parameters in both the measurements and the models. Third, they compared their results to several different competing models and so were able to make quantitative statements about which models were favored and by how much<sup>4</sup>. See Figure 4.

Unfortunately, the LD measurements of Albrow et al. (2001a) only marginally

---

<sup>3</sup> <http://www.astrouw.edu.pl/~ftp/ogle/ogle2/ews/bul-23.html> (Udalski, Kubiak & Szymański 1997)

<sup>4</sup>I note that this analysis was almost entirely the work of a graduate student, Jin An.

discriminate between models. However, it should be possible in the case of future events to obtain smaller errors in the LD parameters and then to use the methods of Albrow et al. (2001a) to say which models are more correct. A significant remaining obstacle to doing this is that linear LD does not accurately represent stellar profiles, at least those that are predicted in models (Orosz & Hauschildt 2001). Hence, differences between the way the model is sampled theoretically and the way the star is effectively sampled by microlensing, can introduce subtle differences in the linear LD coefficient. Problems of this sort are probably the main reason that many authors prefer to compare their results directly with the predictions of models, rather than give parameterized measurements (e.g., Jha et al. 2000). However, if LD measurements are to be used to *discriminate among models* (and not just confirm their general superiority over uniform sources), then the comparison must be made in a “space” that is large enough to encompass several models and allows these models to range over parameters that are only partly constrained, such as temperature and surface gravity. An  $(n \times m)$ -dimensional space defined by  $n$  LD parameters in each of  $m$  bands can perform exactly this function (e.g. Albrow et al. 2001a). While there may be other ways achieve this end, none have come to my attention. Hence, it is important to develop a better parameterization than the conventional linear one, or its more general power-law extensions.

Heyrovský (2001) has made a very important advance in this direction with his suggestion to model stellar profiles as a linear combination of basis functions drawn from a principle component analysis (PCA) of an ensemble of models. If the models are even approximately correct, then the PCA analysis will, by construction, generate a more accurate representation of the stellar profile than the traditional LD decomposition. In order to compare two different ensembles of stellar models, it will probably be necessary to extend Heyrovský’s (2001) original idea to make PCA analyses of each.

## 6.2. Full Spectral/Spatial Resolution

Spectroscopic effects in microlensing events were first discussed by Maoz & Gould (1994) and Valls-Gabaud (1995). Valls-Gabaud (1996,1998) modeled the convolution of point-lens microlensing magnification patterns with spatially resolved stellar spectra and argued that it should be possible to reconstruct the 3-dimensional atmospheric profile from a series of spectral measurements. Heyrovský & Loeb

(1997) worked out an efficient algorithm for carrying out such calculations, and Heyrovský, Sasselov & Loeb (1999) applied this method to make detailed predictions of the spectra of a microlensed M giant ( $T = 3750$  K), including both low ( $R = 500$ ) and high ( $R = 500,000$ ) resolution. Most importantly, they focused attention on specific regions of the spectrum, notably the Balmer lines and TiO bands, that would vary relative to the continuum as the microlensing event progressed.

Unfortunately, all of this work proceeded under the assumption that the source would be resolved by a point-mass lens, whereas in practice the overwhelming majority of spectroscopic observations will be of binary-lens caustic crossings (Gaudi & Gould 1999). One reason for this is that point-mass caustic crossings are intrinsically rarer (see § 4.2), but a much deeper problem is that they cannot be reliably predicted. Since the observations require large ( $\gtrsim 4$  m) class telescopes to which individuals do not generally have dedicated access, it is essential that the caustic crossing be predicted in advance. Once a source has entered a binary caustic, it inevitably must exit. Hence one usually has several days to weeks to make general preparations to observe the crossing, and because fold crossings are characterized by an inverse square-root singularity (eq. 10), they can usually be accurately predicted a day or more in advance.

Alcock et al. (1997b) acquired spectra of an M4 giant in the high-magnification event MACHO 95-BLG-30 and saw changes in  $H\alpha$  and TiO near  $6700\text{\AA}$  that they suggested were due to center-to-limb variations in the spectral lines. Lennon et al. (1996) obtained three 30 min exposures during a caustic crossing of a warm ( $T = 6100$  K) dwarf star using the ESO NTT with  $3.3\text{\AA}$  resolution. Although the source was magnified by a factor  $\sim 25$  at the time of the observations (converting the NTT effectively from a 3.6 m to an 18 m telescope), they were unable to discern any differences in profile shapes for the three observations, and hence were not able to use the caustic crossing to resolve the source.

The only microlensing event to be clearly spectroscopically resolved to date was EROS BLG-2000-5, in which a K3 giant source traversed a binary-lens caustic. In fact, this required the coordinated efforts of 3 microlensing collaborations plus a number of unaffiliated individuals. The event was initially alerted by the EROS

collaboration<sup>5</sup> in April 1999. On 8 June, the MPS collaboration<sup>6</sup> issued an anomaly alert saying the magnification had jumped, and this alert enabled the PLANET collaboration<sup>7</sup> to obtain dense coverage of the first crossing. Because first crossings are not usually predictable, such coverage is extremely rare. Using their precise characterization of the first crossing as well as their detailed measurements of the intra-caustic light curve, PLANET was able to reliably predict not only the time but also the *duration* of the second crossing, which latter was an unprecedentedly long 4 days. The long second crossing meant that the spectra should be taken on successive nights, and so made possible the use of northern as well as southern telescopes. In the end, low-resolution ( $R \sim 1000$ ) spectra were taken from the VLT on four successive nights (Albrow et al. 2001b) and high-resolution ( $R \sim 40,000$ ) spectra were taken from Keck on two successive nights (Castro et al. 2001). Both initial papers focused on  $H\alpha$ . Albrow et al. (2001b) showed that the equivalent width (EW) of this line (which was unresolved) varied during the four nights in the sense of being larger when hotter parts of the stellar surface were more highly magnified, and in particular that it dropped dramatically ( $\sim 25\%$ ) on the last night when only the extreme limb was highly magnified. Although Albrow et al. (2001b) do not mention it, such a sharp drop would imply that the outer  $\sim 4\%$  of the source is strongly in *emission* in  $H\alpha$ , which would be in significant conflict with the atmosphere model that they present. Castro et al. (2001) measured an EW difference in  $H\alpha$  between the two nights of  $8.3 \pm 0.7\%$  and showed that the optical depth difference is roughly constant over the  $\sim 15$  resolution elements that span the line. See Figure 5. The declines in EW between July 6 and 7 measured by the two groups are roughly consistent with one another, although the absolute normalization of the Albrow et al. (2001b) EW is about 10% higher, perhaps reflecting blending of  $H\alpha$  in the low resolution spectrum with a line  $\sim 1 \text{ \AA}$  longward of  $H\alpha$  (see Fig. 2 of Castro et al. 2001).

At present, it is not known exactly what can be learned about stellar atmospheres from studying microlensed spectra. As mentioned above, modeling has been mostly focused on point-mass caustic crossings, whereas it is mostly binary caustics that will be observed spectroscopically. Moreover, the theoretical studies

---

<sup>5</sup><http://www-dapnia.cea.fr/Spp/Experiences/EROS/alertes.html>

<sup>6</sup><http://bustard.phys.nd.edu/MPS/index.html>

<sup>7</sup><http://thales.astro.rug.nl/~planet/>

carried out to date have not examined whether different theoretical atmospheres predict detectably different microlensed spectra. EROS BLG-2000-5 presents a unique opportunity for theorists to compare competing atmosphere models with two excellent data sets to determine whether these distinguish between models. Such a comparison would in turn give important clues as to how to carry out observations of future caustic crossings.

### 6.3. Microlenses as Telescopes

Microlensing events can be used simply as a method to amplify the light gathering capabilities of one's telescope and so obtain deeper spectra than would otherwise be possible. This approach was first applied by Bennetti, Pasquini & West (1995) who were able to type and measure the radial velocity ( $-400 \text{ km s}^{-1}$ ) of a  $V = 20$  K0 subgiant using 3.6 m telescopes at low resolution.

Although, Lennon et al. (1996) failed to resolve the source (see §6.2), they were able to use their magnification  $\sim 25$  observations to measure the temperature and metallicity ( $[\text{Fe}/\text{H}] \sim +0.3$ ) of a bulge dwarf star.

Minnitti et al. (1998) obtained the first high-resolution ( $R = 27,000$ ) spectrum of a microlensing event, MACHO 97-BLG-45, and so by making use of the high magnification were able to obtain the first lithium abundance measurement for a bulge dwarf.

In addition, for several microlensing events, spectra were taken while the source was magnified in order to better characterize the microlensing event itself (Albrow et al. 1998,1999a).

### 6.4. Other Effects

A number of other effects have been proposed that would probe various aspects of the atmospheres of stars, although these have not been met with the same level of interest from observers.

Gould (1997), inverting an idea of Maoz & Gould (1994) showed that spectra taken during a point-lens caustic crossing could be used to measure rotation, even

when the rotational broadening was far smaller than the turbulent broadening.

Simmons, Willis & Newsam (1995) demonstrated that stellar polarization could be measured during a point-lens caustic crossing, even for a radially symmetric polarization field. Of course, in the absence of microlensing, no such effects would be observable for an unresolved source. A number of studies were then carried out for more complicated geometries (Simmons, Newson & Willis 1995; Algol 1996; Belokurov & Sazhin 1997)

Finally, Igance & Hendry (1999), Han et al. (2000) Heyrovský & Sasselov (2000), and Bryce & Hendry (2001), have studied the detection of stellar spots when a source transits either a point-lens caustic or a fold caustic.

## 7. Conclusions

Microlensing has emerged as a powerful probe of stellar astrophysics. The problem of how to use microlensing to measure the stellar MF (including dark objects, BDs, WDs, NSs, BHs) has been solved theoretically, and the practical instrument that can make these measurements, *SIM*, is being built. *SIM* can also be used to make  $\sim 1\%$  measurements of a few dozen nearby stars, which would provide a precision test of stellar models. Both of these prospects still lie almost a decade in the future, but on other fronts, microlensing is already beginning to have an impact on stellar astrophysics. A significant number of binary events have been observed and characterized, and these could already be used to constrain the companion mass-ratio distribution for bulge stars. To date, there have been four LD measurements using microlensing, including one that was very precise, and another that was of a metal-poor A star in another galaxy. And very recently, highly coordinated efforts of the microlensing community have produced the first spatially-resolved spectroscopic measurements of a star other than the Sun. These are impressive accomplishments for a field that, a decade ago, was thought of only in terms of studying dark matter.

**Acknowledgements:** I thank Scott Gaudi for many useful comments and criticisms of the original manuscript. This work was supported in part by grant AST 97-27520 from the NSF and in part by a grant from Le Ministère de l'Éducation Nationale de la Recherche et de la Technologie.

## REFERENCES

- Afonso, C. et al. 2000, *ApJ*, 532, 340
- Albrow, M. et al. 1998, *ApJ*, 512, 672
- Albrow, M. et al. 1999a, *ApJ*, 522, 1011
- Albrow, M. et al. 1999b, *ApJ*, 522, 1022
- Albrow, M. et al. 2000, *ApJ*, 534, 894
- Albrow, M. et al. 2001a, *ApJ*, 549, 759 (astro-ph/0004243)
- Albrow, M. et al. 2001b, *ApJ* 550, L173 (astro-ph/0011380)
- Alcock, C., et al. 1995, *ApJ*, 454, L125
- Alcock, C., et al. 1997a, *ApJ*, 479, 119
- Alcock, C., et al. 1997b, *ApJ*, 491, 436
- Alcock, C., et al. 1998, *ApJ*, 499, L9
- Alcock, C., et al. 2000a, *ApJ*, 541, 270
- Alcock, C., et al. 2000b, *ApJ*, 541, 734
- Alcock, C., et al. 2000c, *ApJ*, 542, 281
- Algol, E. 1996, *MNRAS*, 279, 571
- Baruffolo, A., Benacchio, L., & Benfante, L. 1999, *Astronomical Data Analysis Software and Systems VIII*, ed. D.M. Mehringer, ASP Conference Series, 172, 237 (San Francisco: ASP)
- Belokurov, V.A., & Sazhin, M.V. 1997, *Astronomy Reports*, 41 777
- Benetti, S., Pasquini, L., & West, R.M. 1995, *A&A*, 294, L37
- Bennett, D.P., et al. 1997, *BAAS*, 191, 8303
- Binney, J., Bissantz, N., & Gerhard, O. 2000, *ApJ*, 537, L99
- Boden, A.F., Shao, M., & Van Buren, D. 1998 *ApJ*, 502, 538
- Bogdanov, M.B., & Cherepashchuk, A.M. 1995, *ARep*, 39, 779
- Boutreux, T., & Gould, A. 1996, *ApJ*, 462, 705
- Bryce, H.M., & Hendry, M.A. 2001, in *Microlensing 2000: A New Era in Microlensing Astrophysics*, eds. J.W. Menzies & P.D. Sackett, ASP Conf. Series, in press (astro-ph/0004250)

- Burns, D., et al. 1997, MNRAS, 209, L11
- Castro, S.M., Pogge, R.W., Rich, R.M., DePoy, D.L., & Gould, A. 2001, ApJ 548, L197
- Chang, K. 1981, The Two-Body Gravitational Lens Effect, Ph.D. Thesis, (Hamburg: Univ. of Hamburg)
- Chang, K., & Han, C. 1999, ApJ, 525, 434
- Chang, K., & Refsdal, S. 1979, Nature, 282, 561
- Chang, K., & Refsdal, S. 1984, A&A, 130, 157
- Claret, A., Díaz-Cordovés, J., & Giménez, A. 1995, A&AS, 114, 247
- Claret, A. 1998, A&A, 335, 647
- Deeg, H.J., Garrido, R., & Claret, A. 2001, New Astronomy, in press (astro-ph/0012435)
- Derue, F. 1999, A&A, 351, 87
- Díaz-Cordovés, J., Claret, A., & Giménez, A. 1995, A&AS, 110, 329
- Di Stefano, R., & Mao, S. 1996, ApJ, 457, 93
- Dominik, M. 1998, A&A, 329, 361
- Dominik, M. 1999, A&A, 349, 108
- Dominik, M., & Sahu, K.C. 2000, ApJ, 534, 213
- Duquennoy, A., & Mayor, M. 1991, A&A, 248, 485
- Einstein, A. 1936, Science, 84, 506
- Froeschle, M., Mignard, F., & Arenou, F. 1997, Proceedings of the ESA Symposium 'Hipparcos – Venice '97', p. 49, ESA SP-402
- Gaudi, B.S., & Gould, A. 1997a, 477, 152
- Gaudi, B.S., & Gould, A. 1997b, 483, 83
- Gaudi, B.S., & Gould, A. 1999, 513, 619
- Gaudi, B.S., Naber, R.M., & Sackett, P.D. 1998, ApJ, 502, L33
- Gould, A. 1992, ApJ, 392, 442
- Gould, A. 1994a, ApJ, 421, L71
- Gould, A. 1994b, ApJ, 421, L75



- Gould, A. 1994c, ApJ Letters, submitted, (astro-ph/9408060)
- Gould, A. 1995, ApJ, 441, L21
- Gould, A. 1996, PASP, 108, 465
- Gould, A. 1997, ApJ, 483, 98
- Gould, A. 2000a, ApJ, 532, 936
- Gould, A. 2000b, ApJ, 535, 928
- Gould, A. 2000c, ApJ, 542, 785
- Gould, A. 2001, in *Microensing 2000: A New Era in Microensing Astrophysics*, eds. J.W. Menzies & P.D. Sackett, ASP Conf. Series, in press (astro-ph/0004042)
- Gould, A., & Andronov, N. 1999, ApJ, 516, 236
- Gould, A., Bahcall, J.N. & Flynn, C. 1997, ApJ, 482, 913
- Gould, A., & Han, C. 2000, ApJ, 538, 653
- Gould, A., & Salim, S. 1999, ApJ, 524, 794
- Gould, A., & Welch, D.L. 1996, ApJ, 464, 212
- Griest, K. et al. 1991, ApJ, 372, L79
- Han, C. 1997, ApJ, 484, 555
- Han, C. 2001, MNRAS, in press (astro-ph/0010557)
- Han, C., Chun, M.-S., & Chang, K. 1999, ApJ, 526, 405
- Han, C., Park, S.-H., Kim, H.-I., & Chang, K. 2000, MNRAS, 316, 665
- Han, C., & Gould, A. 1996, ApJ, 467, 540
- Han, C., & Gould, A. 1997, ApJ, 480, 196
- Han, C., & Kim, H.-I. 2000, ApJ, 528, 687
- Hardy, S.J., & Walker, M.A. 1995, MNRAS, 276, L79
- Henry, T.J., & McCarthy, D.W.Jr. 1993, AJ, 106, 773
- Heyrovský, D., 2001, ApJ, submitted
- Heyrovský, D., & Loeb, A. 1997, ApJ, 490, 38
- Heyrovský, D., & Sasselov, D. 2000, ApJ, 529, 69
- Heyrovský, D., Sasselov, D., & Loeb, A. 1999, ApJ, submitted (preprint astro-ph/9902273)

- Hog, E., Novikov, I.D., & Polnarev, A.G. 1995 *A&A*, 294, 287
- Honma, M. 1999, *ApJ*, 517, L35
- Jha, S., Charbonneau, D., Garnavich, P.M., Sullivan, D.J., Sullivan, T., Brown, T.M., & Tonry, J.L. 2000, *ApJ*, 540, L45
- Ignace, R., & Hendry, M.A. 1999, *A&A*, 341, 201
- Kiraga, M. & Paczyński, B. 1994, *ApJ*, 430, 101
- Kuijken, K. 1997, *ApJ*, 486, L19
- Lasserre, T.L., et al. 2000, *A&A*, 355, L39
- Lennon, D.J., Mao, S., Fuhrmann, K., & Gehren, T. 1996, *ApJ*, 471, L23
- Loeb, A., & Sasselov, D. 1995, *ApJ*, 449, L33
- Luyten, W.J. 1979, *New Luyten Catalogue of Stars with Proper Motions Larger than Two Tenths of an Arcsecond (NLTT)* (Minneapolis: Univ. Minnesota Press)
- Luyten, W.J. 1980, *New Luyten Catalogue of Stars with Proper Motions Larger than Two Tenths of an Arcsecond (NLTT)* (Minneapolis: Univ. Minnesota Press)
- Mao, S. 1999, *A&A*, 350, L19
- Mao, S., & Paczyński, B. 1996, *ApJ*, 473, 57
- Maoz, D., & Gould, A. 1994, *ApJ*, 425, L67
- Minniti, D., Vandehei, T., Cook, K. H., Griest, K., & Alcock, C. 1998, *ApJ*, 499, L175
- Miralda-Escudé, J. 1996, *ApJ*, 470, L113
- Monet, D. 1998, *BAAS*, 193, 120.03
- Miyamoto, M., & Yoshii, Y. 1995, *AJ*, 110, 1427
- Nemiroff, R.J. & Wickramasinghe, W.A.D.T. 1994, *ApJ*, 424, L21
- Orosz, J.A., & Hauschildt, P.H. 2001, *A&A*, in press, (astro-ph/0010114)
- Paczyński, B. 1986, *ApJ*, 304, 1
- Paczyński, B. 1991, *ApJ*, 371, L63
- Paczyński, B. 1995, *Acta Astronomica*, 45, 345

- Paczynski, B. 1998, *ApJ*, 494, L23
- Peale, S.J. 1998, *ApJ*, 509, 177
- Peale, S.J. 1999, *ApJ*, 524, L67
- Popowski, P., et al. 2001, in *Microlensing 2000: A New Era in Microlensing Astrophysics*, eds. J.W. Menzies & P.D. Sackett, ASP Conf. Series, in press
- Popper, D.M. 1984, *AJ*, 89, 132
- Refsdal, S. 1964, *MNRAS*, 128, 295
- Refsdal, S. 1966, *MNRAS*, 134, 315
- Rhie, S.H. 1997, *ApJ*, 484, 63
- Rhie, S.H., & Bennett, D.B. 1999, preprint (astro-ph/9912050)
- Salim, S., & Gould, A. 2000, *ApJ*, 539, 241
- Salim, S., & Gould, A. 2001, in preparation
- Sahu, K.C., Chaney, E., Graham, J., Kane, S., & Wieldt, D. 1998, *BAAS*, 192.0701
- Schneider, P., Ehlers, J., & Falco, E.E. 1992, *Gravitational Lenses* (Berlin: Springer)
- Schneider, P., & Weiss, A. 1986, *A&A*, 164, 237
- Schneider, P., & Weiss, A. 1987, *A&A*, 171, 49
- Simmons, J.F.L., Newsam, A.M., & Willis, J.P. 1995, *MNRAS*, 276, 182
- Simmons, J.F.L., Willis, J.P., & Newsam, A.M. 1995, *A&A*, 293, L46
- Soszyński, I., et al. 2001, *ApJ*, in press (astro-ph/0012144)
- Twigg, L.W., & Rafert, J.B., 1980, *MNRAS*, 193, 773
- Udalski, A., Szymanski, M., Kaluzny, J., Kubiak, M., Krzeminski, W., Mateo, M., Preston, G.W., & Paczynski, B. 1993, *Acta Astronomica*, 43, 289
- Udalski, A., et al. 1994, *Acta Astronomica* 44, 165
- Udalski, A., Kubiak, M. & Szymański, M. 1997, *Acta Astronomica*, 47, 319
- Valls-Gabaud, D. 1995, in *Large Scale Structure in the Universe*, ed. J.P. Mücke, S. Gottlöber, & V. Müller (Singapore: World Scientific), 326
- Valls-Gabaud, D. 1996, in *IAU Symposium 173, Astrophysical Applications of Gravitational Lensing*, eds. C.S. Kochanek & J.N. Hewitt (Dordrecht: Kluwer), 237

- Valls-Gabaud, D. 1998, MNRAS, 294, 747
- van Belle, G.T. 1999, PASP, 111, 1515
- van Hamme, W. 1993, AJ, 106, 2096
- Walker, M.A. 1995, ApJ, 453, 37
- Wilson, R.E., & Devinney, E.J. 1971, ApJ, 166, 605
- Witt, H.J. 1990, A&A, 236, 311
- Witt, H.J. 1995, ApJ, 449, 42
- Witt, H.J. & Mao, S. 1994, ApJ, 429, 66
- Zhao, H. S., Spergel, D.N., & Rich, R.M. 1995, ApJ, 440, L13
- Zoccali, M., S., Cassisi, S., Frogel, J.A., Gould, A., Ortolani, S., Renzini, A., Rich, R.M. 1999, & Stephens, A. 2000, ApJ, 530, 418

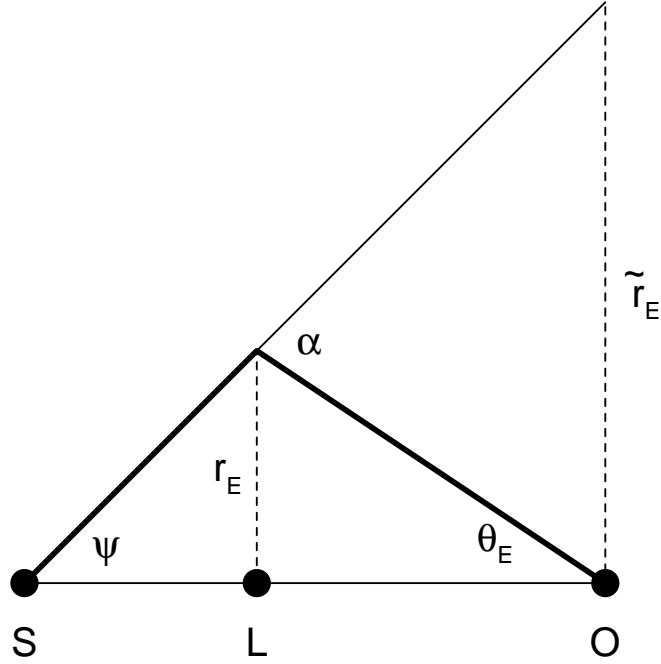


Fig. 1.— Microlensing geometry. Bold curve shows the path of the light from the source (S) to the observer (O) being deflected by the lens (L) of mass  $M$ . The deflection angle is  $\alpha = 4GM/r_E c^2$ , where  $r_E$  is the Einstein radius shown as a dashed line. The image is displaced from the source by the angular Einstein radius  $\theta_E$ . The Einstein radius projected onto the observer plane is  $\tilde{r}_E$ . This diagram allows one to see immediately the relations between the observables ( $\theta_E, \tilde{r}_E$ ) and the physical parameters ( $M, \pi_{\text{rel}}$ ). First, under the small-angle approximation,  $\alpha/\tilde{r}_E = \theta_E/r_E$ , so  $\tilde{r}_E \theta_E = \alpha r_E = 4GM/c^2$ . Second, by the exterior-angle theorem,  $\theta_E = \alpha - \psi = \tilde{r}_E/D_L - \tilde{r}_E/D_S$ , where  $D_L$  and  $D_S$  are the distances to the lens and source. Hence,  $\theta_E/\tilde{r}_E = \pi_{\text{rel}}/\text{AU}$ , where  $\pi_{\text{rel}}$  is the lens-source relative parallax. From Gould (2000c). Copyright American Astronomical Society, reproduced with permission.

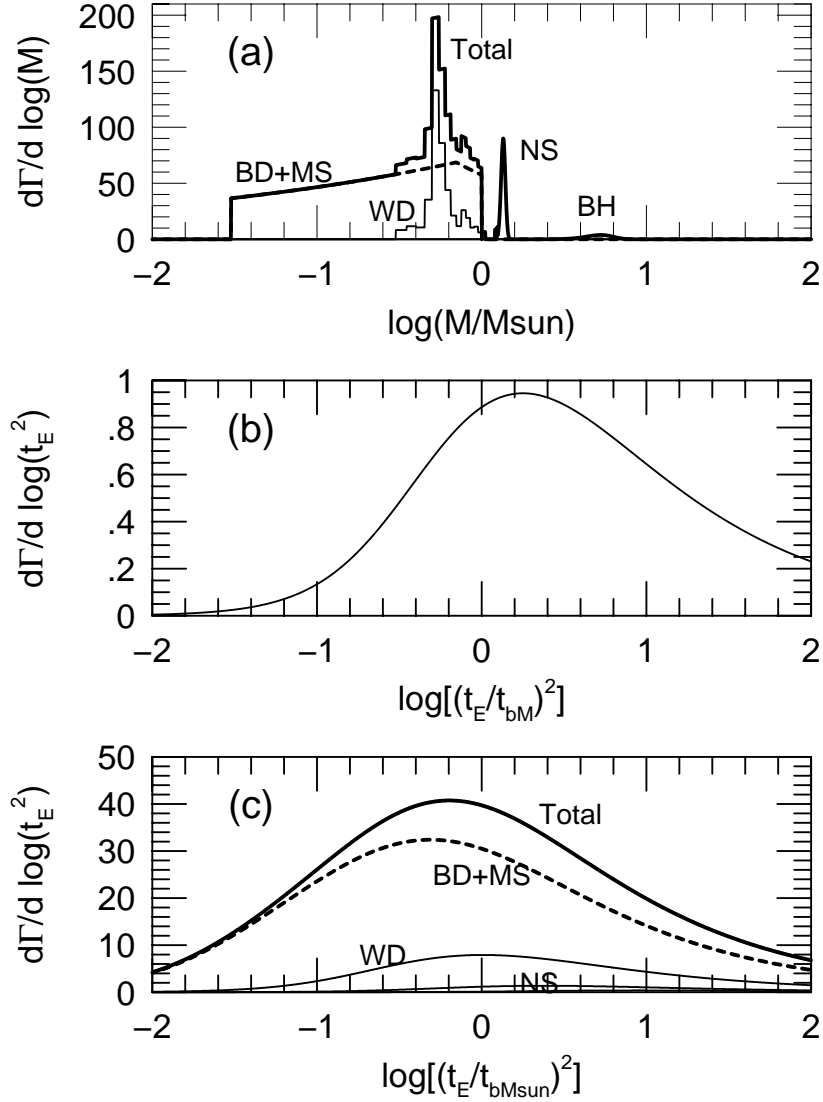


Fig. 2.— Rates of microlensing events toward the bulge by mass (panel *a*) and time scale (panel *c*) for MS+BDs ( $0.03 M_{\odot} < M < 1 M_{\odot}$ ) (*bold dashed curve*) and WD, NS, and BH remnants (*solid curves*). The total is shown by a *bold solid curve*. The mass model (*a*) is described in § 2 of Gould (2000b). It is convolved with the time scale distribution at fixed mass (*b*) derived in § 2.2 of Gould (2000b), to produce the observable time scale distribution (*c*). All three classes of remnants are clearly identifiable in the mass distribution which could be extracted from SIM observations, but are utterly lost in the time scale distribution. The normalizations in panels (*a*) and (*c*) are for 100 events. Panel (*b*) is normalized to unity. From Gould (2000b). Copyright American Astronomical Society, reproduced with permission.

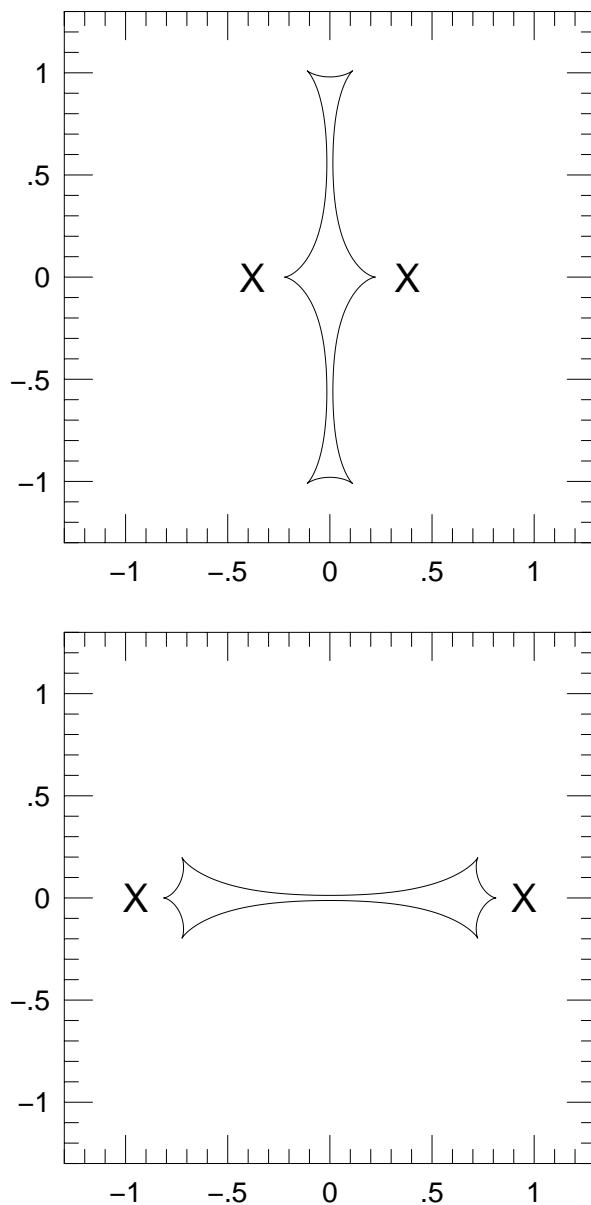


Fig. 3.— Two extreme examples of 6-cusp caustics generated by equal mass binaries. The tick marks are in units of Einstein radii. In each case, the crosses show the positions of the two components. The upper panel shows a relatively close binary with the components separated by  $d = 0.76$  Einstein radii. For  $d < 2^{-1/2}$  the caustic would break up into three caustics, a central 4-cusp caustic plus two outlying 3-cusp caustics. The lower panel shows a relatively wide binary with  $d = 1.9$ . For  $d > 2$  the caustic would break up into two 4-cusp caustics. From Gould (2001). Copyright Astronomical Society of the Pacific, reproduced with permission.

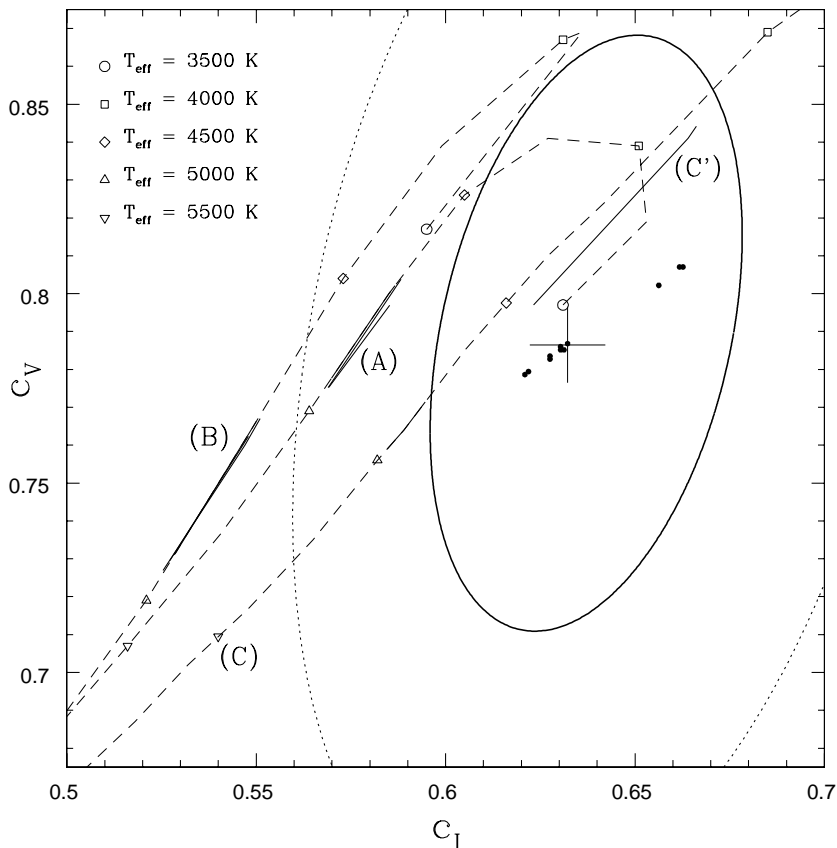


Fig. 4.— Comparison of linear limb-darkening coefficients in  $V$  and  $I$  derived from stellar models and microlensing data for the G/K bulge subgiant in OGLE 2000-BUL-23. The measured value from the best model is represented by a small cross. One (*solid line*) and two (*dotted line*)  $\sigma$  error ellipses are also shown. Small dots are the results with different global ( $d, q$ ) parameters. Various model predictions are displayed by dashed lines ( $\log g = 3.5$ ). Model (A) is taken from Díaz-Cordovés et al. (1995) and Claret et al. (1995), (B) is from van Hamme (1993), and (C) is from Claret (1998). In particular, the predicted values in the temperature range that is consistent with the source color measurement ( $T_{\text{eff}} = [4820 \pm 110]$  K for  $\log g = 3.0$ ;  $T_{\text{eff}} = [4830 \pm 100]$  K for  $\log g = 3.5$ ; and  $T_{\text{eff}} = [4850 \pm 100]$  K for  $\log g = 4.0$ ) are emphasized by thick solid lines. Model (C') is by Claret (1998) for stars of  $T_{\text{eff}} = (4850 \pm 100)$  K for  $\log g = 4.0$ . Although the measured value of the limb-darkening coefficients alone favors this model, the required young age would imply a disk rather than bulge source, which would be inconsistent with the lens-source relative proper motion measured for this event. From Albrow et al. (2001a). Copyright American Astronomical Society, reproduced with permission.



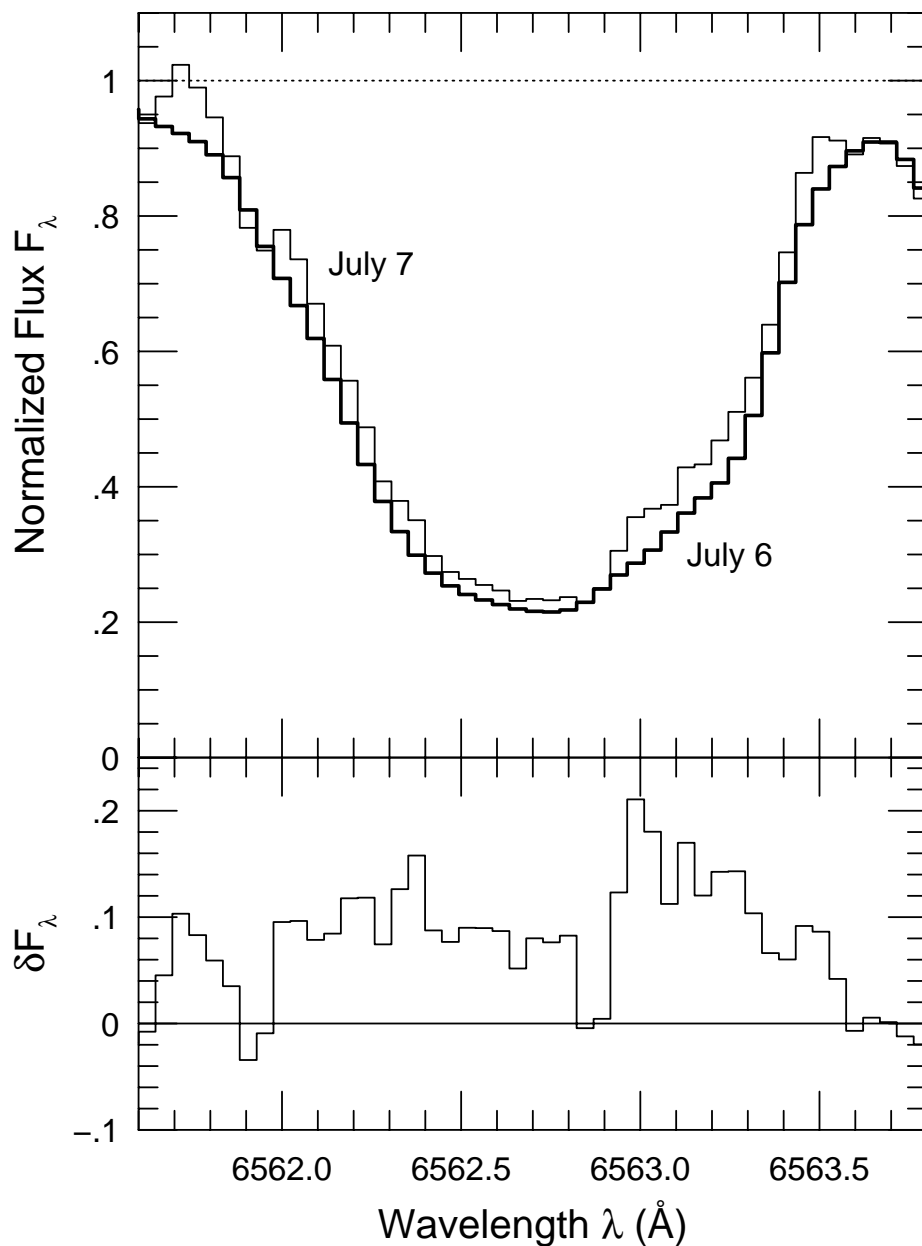


Fig. 5.— Upper panel: Keck HIRES spectra of a K3 bulge giant taken during the binary-lens caustic crossing of EROS BLG-2000-5 on the nights of 6 July (*bold*) and 7 July (*solid*) 2000. Only the  $H\alpha$  line at  $\lambda = 6562.7\text{\AA}$  is shown. The full spectrum covers the range  $5500\text{\AA} < \lambda < 7900\text{\AA}$ . The equivalent width of  $H\alpha$  is  $8.7 \pm 0.7\%$  smaller on the second night. The spectra have each been normalized to a continuum of unity and have been convolved to the same resolution. Lower panel: Fractional difference in the lines between the two nights as a function of wavelength,  $\delta F_\lambda \equiv 2(F_6 - F_7)/(F_6 + F_7)$ , where  $F_6$  and  $F_7$  are the normalized fluxes from July 6 and July 7 respectively. From Castro et al. (2001). Copyright American Astronomical Society, reproduced with permission.